Open access • Journal Article • DOI:10.1111/J.1365-2486.2009.01908.X

Remote sensing of sun-induced fluorescence to improve modeling of diurnal courses of gross primary production (GPP) — Source link

Alexander Damm, Jan Elbers, André Erler, Beniamino Gioli ...+13 more authors

Institutions: Humboldt University of Berlin, Forschungszentrum Jülich, University of Milan, University of Valencia ...+1 more institutions

Published on: 01 Jan 2010 - Global Change Biology (Wiley-Blackwell)

Remote sensing of sun-induced fluorescence to improve modeling of diurnal courses of gross primary production (GPP)

Damm, A; Erler, A; Gioli, B; Hamdi, K; Hutjes, R; Kosvancova, M; Meroni, M; Miglietta, F; Moersch, A; Moreno, J; Schickling, A; Sonnenschein, R; Udelhoven, T; van der Linden, S; van der Tol, C; Hostert, P; Rascher, U

This is the pre-peer review version of the following article:

DAMM, A., ELBERS, J., ERLER, A., GIOLI, B., HAMDI, K., HUTJES, R., KOSVANCOVA, M., MERONI, M., MIGLIETTA, F., MOERSCH, A., MORENO, J., SCHICKLING, A., SONNENSCHEIN, R., UDELHOVEN, T., VAN DER LINDEN, S., HOSTERT, P. & RASCHER, U. (2009): Remote sensing of sun induced fluorescence to improve modelling of diurnal courses of Gross Primary Production (GPP). Global Change Biology, doi: *10.1111/j.1365-2486.2009.01908.x.*

REMOTE SENSING OF SUN INDUCED FLUORESCENCE TO IMPROVE MODELLING OF DIURNAL COURSES OF GROSS PRIMARY PRODUCTION (GPP)

Alexander Damm[1], Jan Elbers[2], André Erler[3], Beniamino Gioli[4], Karim Hamdi[3], Ronald Hutjes[2], Martina Kosvancova[5], Michele Meroni[6], Franco Miglietta[4], André Moersch[3], Jose Moreno[7], Anke Schickling[8], Ruth Sonnenschein[1], Thomas Udelhoven[9], Sebastian van der Linden[1], Patrick Hostert[1], Uwe Rascher[3]

[1]Geomatics Lab, Humboldt-Universität zu Berlin, Unter den Linden 6, 10099 Berlin, Germany

[2]Alterra, Duivendaal 2, 6701 AP Wageningen, The Netherlands

[3]Institute of Chemistry and Dynamics of the Geosphere, ICG-3: Phytosphere, Forschungszentrum Jülich, Stetternicher Forst, 52425 Jülich, Germany

[4]IBIMET-CNR, Istituto di Biometeorologia, Consiglio Nazionale delle Ricerche, Via G. Caproni 8, 50145 Firenze, Italy

[5]Laboratory of Plants Ecological Physiology, Division of Ecosystem Processes, Institute of Systems Biology and Ecology, Poříčí 3b, 60300 Brno, Czech Republic

[6]Remote Sensing of Environmental Dynamics Lab., DISAT, University of Milan-Bicocca, Piazza della Scienza 1, 20126 Milano, Italy

[7]Department of Earth Physics and Thermodynamics, University of Valencia, Dr Moliner, 50, 46100 Burjassot - Valencia, Spain

[8]Institute for Geophysics and Meteorology, University of Cologne, Kerpener Str. 13, 50937 Cologne, Germany

[9]CRP-Gabriel Lippmann, Département 'Environnement et Agro-biotechnologies', Geomatic Platform, 41, rue du Brill, 4422 Belvaux, Luxembourg

[*] Corresponding author: alexander.damm@geo.uzh.ch; phone +41 (0) 44 635 5251

Abstract

Terrestrial gross primary production (GPP) is an important parameter to explore and quantify carbon fixation by plant ecosystems at various scales. Remote sensing offers a unique possibility to investigate GPP in a spatially explicit fashion; however, budgeting of terrestrial carbon cycles based on this approach still remains uncertain. To improve calculations, spatio-temporal variability of GPP must be investigated in more detail on local and regional scales. The overarching goal of this study is to enhance our knowledge on how environmentally induced changes of photosynthetic light use efficiency (LUE) are linked with optical remote sensing parameters. Diurnal courses of sun-induced fluorescence yield (FS_{yield}) and the Photochemical Reflectance Index (PRI) of corn were derived from high resolution spectrometric measurements and their potential as proxies for LUE was investigated. GPP was modeled using Monteith`s LUE-concept and optical based GPP and LUE values were compared to synoptically acquired eddy covariance data. It is shown that the diurnal response of complex physiological regulation of photosynthesis can be tracked reliably with the sun-induced fluorescence. Considering structural and physiological effects, this research shows for the first time that including sun-induced fluorescence into modeling approaches improves their results in predicting diurnal courses of GPP. Our results support the hypothesis that air or spaceborn quantification of sun-induced fluorescence yield may become a powerful tool to better understand spatio-temporal variations of fluorescence yield, photosynthetic efficiency and plant stress on a global scale.

Keywords

GPP, sun-induced fluorescence, fluorescence yield, PRI, eddy covariance, diurnal carbon uptake, LUE, remote sensing, spectroscopy

List of abbreviations

Acronym	Abbreviation	Unit
A_{max}	maximum assimilation rate of CO_2	µmol CO_2 m^{-2} s^{-1}
APAR	absorbed photosynthetic active radiation	µmol m^{-2} s^{-1}
CEFLES2	joint ESA campaign for the projects CarboEurope, Fluorescence Explorer, Sentinel2	
Chl-F	chlorophyll fluorescence	
CO_2	carbon dioxide	
EC	eddy covariance	
ESA	European Space Agency	
ETR	photosynthetic electron transport rate	µmol m^{-2} s^{-1}
ETR_{PAM}	electron transport rate measured with PAM fluorometer	µmol m^{-2} s^{-1}
fAPAR	fraction of absorbed photosynthetic active radiation	%
FLD	Fraunhofer line discrimination	
F_T	terminal fluorescence measured with PAM fluorometer	a.u.
F_O	minimum fluorescence measured with PAM fluorometer	a.u.
$F_{M'}$	maximum fluorescence of light adapted leaf measured with PAM fluorometer	a.u.
F_M	maximum fluorescence of dark adapted leaf measured with PAM fluorometer	a.u.
F_v	variable fluorescence of dark adapted leaf measured with PAM fluorometer	a.u.
F_v/F_M	maximum quantum yield of PSII of dark adapted leaf	a.u.
FOV	field of view	
F_S	sun-induced fluorescence measured with spectrometer	µmol m^{-2} s^{-1}
F_{Syield}	fluorescence yield measured with spectrometer	a.u.
G	ground heat flux	W/m²
G_s	stomatal conductance	mol H_2O m^{-2} s^{-1}
GPP	gross primary production	µmol m^{-2} s^{-1}
GPP_{EDDY}	gross primary production measured with eddy flux tower	µmol m^{-2} s^{-1}
GPP_{PRI}	gross primary production modeled with PRI	µmol m^{-2} s^{-1}
GPP_{FS}	gross primary production modeled with sun induced fluorescence	µmol m^{-2} s^{-1}
$GPP_{Fsyield}$	gross primary production modeled with fluorescence yield	µmol m^{-2} s^{-1}
GPP_{const}	gross primary production modeled with a constant LUE	µmol m^{-2} s^{-1}
H	sensible heat flux	W m^{-2}
H_2O	water	
JCO_2	leaf-level CO_2 assimilation rate measured using the clip-on LICOR gas-exchange analyzer	µmol m^{-2} s^{-1}
LAD	leaf angle distribution	
LAI	leaf area index	m^2 m^{-2}
LE	latent heat flux	W m^{-2}
LED	light emitting diode	
LUE	light use efficiency	mol CO_2 mol^{-1} photons
LUE_{EDDY}	light use efficiency derived from eddy flux data	mol CO_2 mol^{-1} photons
LUE_{LICOR}	light use efficiency derived with LICOR gas-exchange analyzer	mol CO_2 mol^{-1} photons
LUE_{PAM}	actual quantum efficiency or quantum yield of PS II measured with PAM fluorometer	
NEE	net ecosystem exchange	µmol m^{-2} s^{-1}
NPQ	non photochemical quenching	
O_2	oxygen	
PPFD	photosynthetic photon flux density	µmol m^{-2} s^{-1}
PRI	Photochemical Reflectance Index	
R_{eco}	ecosystem respiration rate	µmol m^{-2} s^{-1}

PS I	photosystem I	
PS II	photosystem II	
RMSE	root mean square error	
Rn	net radiation	$W\ m^{-2}$
RS	Remote sensing	
u*	friction velocity	$m\ s^{-1}$
VPD	vapor pressure deficit	kPa

1 Introduction

Up to 90% of the gas exchange between the terrestrial bio-geosphere and the atmosphere is mediated by plants (Ozanne et al. 2003). Thereby, approximately 60 Gt of carbon are annually absorbed through plant photosynthesis (Janzen 2004). Slight alterations within the terrestrial carbon balance can have significant impact on atmospheric carbon dioxide (CO_2) concentrations (Hilker *et al.* 2008b). In consequence, much effort in bio-geoscience research has been put in improving the understanding of CO_2 fluxes at different temporal and spatial scales (Baldocchi 2003, Cohen *et al.* 2003, Turner *et al.* 2003a). Gross Primary Production (GPP) was identified as a key parameter to explore and quantify carbon fixation by plant ecosystems at various scales (Field *et al.* 1995, Goetz & Prince 1999).

Currently, two different data-driven approaches exist to quantify variations in GPP at local or regional scales. (i) The Eddy covariance (EC) technique aims at direct measurements of CO_2 net fluxes above canopies and uses micrometeorological methods to derive CO_2 exchange associated to a spatially extended footprint. (ii) Remote sensing (RS) based approaches aim for air- and spaceborne retrieval of optical parameters that are related to photosynthetic carbon fixation.

An extensive network of EC towers was established during the last few decades. It provides CO_2 flux data from a wide range of plant ecosystems at high temporal resolution (Baldocchi et al. 2001). Recent algorithmic development allows GPP estimates with high accuracy (Goulden *et al.* 1996, Baldocchi 2003). EC towers measure carbon fluxes associated with a footprint area typically in the order of up to ~1 km² depending on local setup and aerodynamic properties. Thus, measurements are local and solely representative for the underlying ecosystem as a whole (Turner *et al.* 2003b, Drolet *et al.* 2008).

RS offers the unique possibility to derive spatially explicit information on local, regional or global scales (Goetz & Prince 1999, Freedman *et al.* 2002, Hilker *et al.* 2008b). Observations

85 of GPP from remote sensing is based on a relationship between spectral reflectance and two
86 key vegetation parameters: the Absorbed Photosynthetic Active Radiation (APAR) and the
87 plant efficiency to utilize this radiation for photosynthesis (Goetz & Prince 1999). Monteith´s
88 (1972, 1977) mechanistic Light Use Efficiency (LUE) concept relates the photosynthetic
89 capacity to LUE [mol CO_2 mol photons^{-1}], defined as biomass production per unit absorbed
90 light. Accordingly, knowing the incident PAR, GPP can be described as a function of the
91 fraction of Absorbed Photosynthetic Active Radiation (fAPAR) and LUE (Turner *et al.*
92 2003a, Hilker *et al.* 2008b). Both parameters are highly variable and depend on phenological
93 status, canopy structure, and species composition (Field *et al.* 1995, Goetz & Prince 1999).
94 While fAPAR is expected to change mainly as a function of sun zenith angle and vegetation
95 cover, LUE is highly dynamic and as a result, insufficient parameterization of this quantity is
96 identified as a main source of uncertainty in modeling GPP (Turner et al. 2003b). In fact,
97 plant photosynthesis is a dynamically regulated process that quickly adapts to environmental
98 conditions and is affected by the ecological plasticity of each species (Turner *et al.* 2003b,
99 Rascher & Nedbal 2006). Consequently, LUE may greatly vary between different species
100 and, additionally, is dynamically adjusted in diurnal and seasonal cycles (Schurr et al. 2006).
101 The observation of GPP from space can principally be grouped into three approaches: (i)
102 methods that link optical vegetation indices to APAR with constant LUE; ii) methods that are
103 similar to the first one while LUE is related to meteorological parameters iii) approaches that
104 estimate both APAR and LUE directly from RS data. The first two groups of methods often
105 yields insufficient results, because they measure only APAR while assuming LUE to be
106 constant or it is modeled from ancillary meteorological variables (Goetz & Prince 1999,
107 Grace *et al.* 2007). In this case, LUE is empirically related to some key meteorological
108 variables such as temperature or vapor pressure deficit, which are selected as proxies for
109 environmental stress (Field *et al.* 1995, Heinsch *et al.* 2002). Some studies show the potential
110 of these approaches to predict GPP on regional and global scale with a temporal resolution of

111 a couple of days (Heinsch *et al.* 2002, Running *et al.* 2004, Coops *et al.* 2007). However, such
112 methods require frequent re-calibration, being a limiting factor for long term monitoring
113 (Turner et al. 2005).
114 Research has recently focused on estimating APAR and LUE directly from RS data because
115 these methods are expected to provide more realistic GPP estimates (Goetz & Prince 1999,
116 Grace *et al.* 2007). The peculiarity of this group of methods is that RS data are used to track
117 the complex physiological process of photosynthesis and its strong dependency on different
118 environmental conditions. The efficiency of photosynthesis is controlled on various levels,
119 e.g. for chloroplasts, cells and leaves, in response to physiological characteristics and
120 environmentally conditions (see Schulze and Caldwell (1995) for a summary on the
121 ecophysiology of photosynthesis). In the case of limited photosynthesis and an increased
122 amount of incident light, this excess energy can lead to photo-oxidative damages of the
123 photosynthetic apparatus (Demmig-Adams & Adams 1996, Baker 2008). Two processes
124 within the photosystem II (PS II) are known in dissipating the destructive energy and
125 protecting the chloroplasts from damages. Fluorescence transforms the excess energy
126 harvested at a given wavelength to emitted light at longer wavelengths (Fs). Non-
127 Photochemical Quenching (NPQ) mechanisms protect the chloroplasts by degrading the
128 excess energy into heat (Demmig-Adams & Adams 1996, Baker 2008).
129 In the past years, relevant advances in sensor technology allowed to quantify LUE indirectly
130 by remotely sensing of the two dissipation pathways - NPQ and fluorescence. The
131 photochemical reflectance index (PRI) was designed to track the NPQ related xanthophyll
132 cycle at leaf level (Gamon *et al.* 1992, Gamon *et al.* 1993). This important process within
133 NPQ has a short response time to variable states of photosynthetic rates. Excessive light
134 conditions induce the de-epoxidation of violaxanthin pigments into antheraxanthin and
135 zeraxanthin - a mechanism reversible under low light conditions. The variable pigment
136 composition leads to changes of the spectral signal at 531 nm (Gamon et al. 1992). PRI has

been used in a variety of case studies and positively correlates with photosynthetic efficiency. It has been used successfully to detect changes in photosynthetic efficiency at the leaf level (see Rascher et al. (2007) for an overview of the literature). However, PRI values greatly vary between species with the same photosynthetic capacity (Guo & Trotter 2004). Additionally, canopy level PRI is strongly affected by viewing and illumination angles, soil background, leaf orientation and leaf area (Barton & North 2001, Hilker *et al.* 2008b). Thus, the suitability of PRI as proxy for LUE in complex canopies remains unclear. Methy (2000) did not find a significant relationship of PRI and LUE at canopy level, whereas some studies have demonstrated the potential of PRI as proxy for LUE (see Hall et al. (2008) for a review on the subject).

Light energy absorbed by photosynthetic pigments is partly re-emitted as Fs, having well defined spectral characteristics. Chlorophyll fluorescence (Chl-F) is emitted in two broad bands with peaks at about 685 and 740 nm (Lichtenthaler & Rinderle 1988, Franck *et al.* 2002). The intensity of the fluorescence signal is in principle inversely correlated to the energy used for photosynthesis and thus can serve as an indicator for photosynthetic light conversion (Baker 2008). However, the inverse correlation is in many cases lost as result of increased rates of NPQ processes that become dominant in dissipating the excess energy (Govindjee 1995) and the exact relationship between NPQ and fluorescence is hard to obtain (Maxwell & Johnson 2000). Since commercial instruments for measuring fluorescence have become available in the past decades, the fluorescence method has been widely used in plant ecophysiological research on the level of single leaves and organs (Schreiber & Bilger 1993, Schreiber *et al.* 1995).

In contrast to a detailed understanding on the level of single leaves, our research focused on investigating fluorescence-based methods for quantifying canopy level GPP, which requires remote analysis from above canopy. Recent studies showed that sun-induced chlorophyll fluorescence can principally be detected using passive techniques (Moya *et al.* 2004, Louis *et*

163 *al.* 2005, Meroni & Colombo 2006) and that remotely derived fluorescence signals and
164 photosynthetic rates can be linked (Freedman *et al.* 2002, Louis *et al.* 2005, Meroni *et al.*
165 2008a, Meroni *et al.* 2008b). However, the sun-induced fluorescence signal and the
166 relationship of fluorescence and LUE are not yet fully understood (Grace et al. 2007).
167 Operational methods solely rely on potential photosynthetic rates that were modified by
168 microclimatological variables. Compared to such methods, approaches based on direct
169 measurements of photosynthetic rates will simplify estimating GPP from remote sensing data.
170 Nevertheless, the measurement of parameters related to photosynthetic capacity with optical
171 parameters is challenging. Hence, the overarching goal of this study is to further improve our
172 understanding of LUE temporal dynamics, their linkage to environmental boundary
173 conditions and the possibility to track these dynamics with optical parameters. Fluorescence
174 yield and PRI were tested as proxies for LUE and their ability to explain short time responses
175 of photosynthetic activity to environmental stress was investigated. Diurnal courses of
176 radiometric measurements were acquired and the optical parameters *sun-induced fluorescence*
177 *yield,* and *PRI* were derived. They were then used to predict GPP based on Monteith's LUE
178 concept and compared to estimates from a local EC tower.
179

180 **2 Materials and methods**

181 **2.1 Study site**

182 Field data were acquired as part of the European Space Agency (ESA) supported CEFLES-2
183 campaign in June and September 2007 (*http://www.esa.int/esaLP/SEMQACHYX3F_*
184 *index_0.html)*. The campaign was carried out in the "Les Landes" area in Southwest France.
185 The main site is located near the commune Marmande, in a plain of the Garonne valley and
186 dominated by intensive agriculture. Main crop types are corn (*Zea mays*), winter wheat
187 (*Triticum vulgare*) and beans (*Phaseilus vulgaris*). An eddy flux tower (LAT/LON 44.464,

188 0.196, altitude 22m above sea level) was installed within a large corn field (500 x 300 m),
189 which was also mainly surrounded by corn fields.
190 The spectral database available for this research contains discontinuous time series of
191 observations. During the first measurement period in June (1 day of measurements), corn was
192 in the growing phase with an average plant height of 2 m. In September, when subsequent
193 measurement periods 2 (3 days) and 3 (1 day) were undertaken, corn plants reached
194 maximum heights of about 3.2 m and were at the beginning of the senescence phase. During
195 both campaigns, the corn field was not irrigated.
196
197 **2.2 Physiological data**
198 ***Leaf level***
199 Leaf-level measurements using a pulse-amplitude-modulated (PAM) fluorometer, a gas
200 exchange analyzer and a chlorophyll meter were taken to verify potential physiological
201 limitations of photosynthesis and to support interpreting canopy signals.
202 *PAM fluorometry in the field*
203 Chlorophyll fluorescence measurements over corn leaves exposed to ambient incident
204 photosynthetic photon flux density (PPFD) were performed with the miniaturized PAM
205 (WALZ 2008) with a leaf clip holder as described by Bilger et al. (1995). Fluorescence was
206 excited by a pulsed modulated red light from a light-emitting-diode (LED), which passes a
207 cut-off filter (λ<670 nm, Balzers DT Cyan, special). Terminal fluorescence (F_T) was
208 determined at ambient light conditions. To determine maximum fluorescence (F_M'), a
209 saturating light pulse (800 ms, ~ 3000 μmol m^{-2} s^{-1}) was superimposed to the ambient light
210 conditions.
211 Measurements were performed on September 13th 2007 for six individual plants in the same
212 field, whereas two leafs per plant were measured from 9:30 h until 15:45 h. The values were
213 aggregated for one hour and 15 min time periods.

214 Actual quantum efficiency of PS II (LUE_{PAM}) (quantum yield of PSII) was calculated
215 according to Genty et al. (1989) as:

216 $$LUE_{PAM} = \frac{F_M' - F_T}{F_M'} = \frac{\Delta F}{F_M'} \quad (1)$$

217 The photosynthetic electron transport rate (ETR_{PAM}) was obtained:

218 $$ETR_{PAM} = \frac{\Delta F}{F_M'} \bullet PPFD \bullet 0.5 \bullet 0.84 \quad (2)$$

219 The use of the factor 0.5 assumes that the incident quanta were used to excite both PS II and
220 PS I. The value 0.84 accounts for the absorption coefficient of leaves. As this factor is not
221 exactly known for corn, we used the empirical mean absorption factor (Ehleringer 1981).
222 PPFD of each leaf area unit was obtained with a leaf clip holder featuring an integrated micro-
223 quantum sensor.

224 Maximum or potential quantum yield of PS II (F_v/F_M) was calculated according to Eq. 3.

225 $$F_v / F_M = \frac{(F_M - Fo)}{F_M} \quad (3)$$

226 F_M donates the maximum fluorescence of the dark-adapted leaf when a saturating light pulse
227 of 800 ms duration (intensity ~ 3000 µmol m^{-2} s^{-1}) was applied.

228 *Gas exchange measurements*

229 Light response curves of CO_2 assimilation rate (JCO_2) were measured using the LED light
230 source Li-6400-02B (LiCor, USA). The values of JCO_2 were recorded with a gas exchange
231 system Li-6400 (LiCor, USA). The irradiances used for the light response curve were 0, 80,
232 250, 600, 1200 and 1800 µmol (photons) m^{-2} s^{-1}. This measuring protocol allowed the
233 estimation of JCO_2 at a given PPFD as half-hour averages of the eddy flux measurements.

234 Measurements were performed on September 12th 2007 from 7:30 h until 17:30 h on four
235 individual plants. The CO_2/H_2O fluxes were measured as an integral signal from the central
236 parts of the leaves (investigated area 6 cm^2) on the 4th leaves from the top. The leaves were
237 kept inside the assimilation chamber under constant CO_2 concentration (380±5 µmol (CO_2)

238 mol^{-1}), air humidity and leaf temperature (outdoor ambient) during the measurement. Air flow
239 rate through the assimilation chamber was maintained at 500 µmol s^{-1}.
240 LUE_{LICOR} was derived as the ratio of JCO_2 and PPFD given as a half-hour average from the
241 eddy flux measurements.
242 *Chlorophyll content*
243 The leaf chlorophyll content was measured with the Chlorophyll Meter SPAD-502 (Spectrum
244 Technologies Inc., USA). The relative measurements of the SPAD device were calibrated
245 using laboratory chlorophyll extractions. For this purpose, leaf disks were cut with a
246 standardized cork borer, placed in plastic tubes and stored in liquid-nitrogen. The chlorophyll
247 content of the leaf samples was extracted in the laboratory using the method after
248 Lichtenthaler (1987).
249
250 ***Canopy Level***
251 Net ecosystem exchange (NEE) was measured half-hourly (EC tower) from April until
252 September 2007 together with friction velocity (u*), energy fluxes and fluxes of trace species.
253 Sensible heat flux (H), latent heat flux (LE), and ground heat flux (G) were measured to
254 calculate the surface energy balance expressed as the distribution of net radiation (Rn).
255 Standard equipment included a 3D sonic anemometer, an infrared gas analyzer measuring
256 CO_2 and gaseous H_2O mass densities at high frequency, a slow response infrared gas analyzer
257 measuring vertical CO_2 concentration profiles at 5 levels up to 20m, a soil heat flux plate, and
258 global and net radiation sensors. u*, H, LE and NEE were calculated using the eddy
259 covariance technique, following the standardized protocol for instrument setup and data
260 processing by Aubinet et al. (2000), including density corrections for open path gas analyzers
261 (Webb et al. 1980).
262 Raw flux data required additional pre-processing for reliable subsequent analyses (Goulden et
263 al. 1996). Three pre-processing steps were performed using a set of algorithms provided by

264 the CarboEurope network (CarboEurope 2008) and described elsewhere (Papale & Valentini
265 2003, Reichstein *et al.* 2005). Since EC measures the NEE (i.e. the sum of CO_2 fixed by
266 plants, GPP, and ecosystem respiration rate, (R_{eco})), the integrated flux signal was partitioned
267 to derive GPP. For this purpose, night-time NEE measurements were used to relate R_{eco} to soil
268 temperature. Day time R_{eco} was obtained with the established relationship and subtracted from
269 the daytime NEE values.
270 Finally, the pre-processed data were smoothed using a 1.5 h moving window filter to reduce
271 data inherent noise (Reichstein *et al.* 2002, Eiden *et al.* 2007). Besides GPP, light use
272 efficiency (LUE_{EDDY}) was calculated as second reference parameter from the EC-data.
273 LUE_{EDDY} was derived as ratio of GPP_{EDDY} and PPFD according to Wofsy et al. (1993).
274

275 **2.3 Remotely sensed data and optical parameters**

276 A FieldSpec Pro III high resolution spectroradiometer (Analytical Spectral Devices, Boulder,
277 USA) (ASD 2002) was installed at 30 m distance to the eddy flux tower to measure diurnal
278 cycles of canopy radiometric response. It registers reflected radiation within the spectral
279 domain of 350-2500 nm with a nominal bandwidth of 1.4 nm (350-1050 nm) and a field-of-
280 view (FOV) of 25°. A calibrated Spectralon™ panel (0.25 x 0.25 m) was used for calibration
281 of the instrument and to measure incident irradiance.

282 The instrument's fiber optic was mounted on a robotic arm of 0.6 m length, approximately 1
283 m above the canopy. Moving the robotic arm allowed an automatic collection of daily cycles
284 of spectral reflectance at four different locations, each of which was 0.5 m in diameter (Fig 1).
285 The acquired dataset consists of spectral records from four canopy areas, bracketed by
286 measurements of the reference panel. At each position, 10 single spectra were recorded and
287 each spectrum was averaged from 25 individual measurements. Integration time was
288 automatically optimized during the day in order to maximize the signal-to-noise ratio.
289

290 figure 1

291

292 Five diurnal courses were acquired during the campaign that covers two different
293 phenological periods, June and September 2008 (Table 1). Measurements acquired in
294 September were collected in two different locations of the same field and therefore they were
295 divided into two datasets and treated separately. Hence, period one corresponds to a single
296 day course in June. Period two consists of three diurnal courses from the 5th to 7th of
297 September. Period three corresponds to measurements from the 12th September at a different
298 position in the same field.

299

300 table 1

301

302 The Photochemical Reflectance Index was introduced by Gamon et al. (1992) to track the
303 epoxidation state of the xanthophyll pigments. The index is based on two wavelengths in the
304 visible spectral domain. The spectral reflectance at 531 nm (R_{531}) is sensitive for pigment
305 variation associated to NPQ while the reflectance at 570 nm (R_{570}) is used as reference. The
306 PRI was derived as:

307 $$PRI = \frac{R_{531} - R_{570}}{R_{531} + R_{570}} \quad (4)$$

308 Reflectance values were calculated using the Spectralon^{TM} reference measurements.
309 The amount of sun-induced chlorophyll fluorescence (F_S) emitted by a sunlit leaf is only 1-
310 5% of the total reflected light at a certain wavelength, which complicates quantifying the
311 fluorescence signal from RS observations. However, the solar light is absorbed in the solar or
312 earth atmosphere at the so called *Fraunhofer lines* and no or strongly reduced incoming
313 radiation reaches the Earth surface. Fluorescence originated in the canopy also occurs in the
314 otherwise 'black' absorption bands and, therefore, can be selectively quantified. Solar

315 irradiance at ground level exhibits three main absorption bands in the red and near infrared
316 spectral domain: the H_α line at 656.3 nm is due to the hydrogen absorption by the solar
317 atmosphere whereas two bands at 687 nm (O_2-B) and 760 nm (O_2-A) are due to the molecular
318 oxygen absorption by the terrestrial atmosphere. Especially the O_2-A and -B bands overlap
319 with the chlorophyll fluorescence emission spectrum and are wide enough to allow
320 quantifying fluorescence from air- and spaceborne platforms. The Fraunhofer Line
321 Discrimination method (FLD) has been proposed for this purpose (Plascyk 1975) and was
322 used with success in different works (Carter *et al.* 1990, Moya *et al.* 2004).
323 In this study, we used the O_2-A band, which is the widest of the three absorption bands
324 (deepest absorption at 760 nm, < 2 nm bandwidth; max bandwidth affected by O_2 absorption
325 ~12 nm), to quantify fluorescence according the modified FLD method proposed by Maier et
326 al. (2003). This approach assumes that F_S is additive to the reflected signal and can be derived
327 by comparing the depth of the oxygen absorption band at 760 nm from a non-fluorescent
328 surface with that of the fluorescent vegetation target according to Eq. 5,

329 $$F_S = \frac{L_1 - \frac{E_1}{E_2} \bullet L_2}{1 - \frac{E_1}{E_2}} \quad (5)$$

330 where E is the radiance up-welling from the non fluorescent target, L is the radiance of
331 vegetation, and the subscripts 1 and 2 indicating the wavelengths within and outside of the
332 absorption line, respectively. We employed the band at 760 nm for E_1 and L_1 and an average
333 of the spectral bands at 745-755 nm and 770-785 nm for E_2 and L_2.
334 Besides responding to photosynthetic status, fluorescence is also driven by the absolute
335 magnitude of the incident irradiance. Hence, it is necessary to normalize the estimated F_S
336 signal to get a fluorescence yield independent of the light level. This can be achieved by
337 dividing the number of photons emitted (F_S) and the number of photons absorbed by the
338 plants (APAR). The resulting signal is termed fluorescence quantum yield (F_{Syield}) (Govindjee

2004) and can be related to the photosynthetic efficiency (Louis et al. 2005) and was obtained according Eq. 6:

$$F_{Syield} = \frac{F_S}{APAR} \quad (6)$$

2.4 GPP modeling

For modeling GPP based on RS data, we used the concept introduced by Monteith (1972, 1977). According to Eq. 7, GPP is a function of APAR and LUE.

$$GPP = APAR \bullet LUE \quad (7)$$

APAR was obtained from the radiometric measurements as integrated difference between the incident and reflected radiance in the spectral region from 400 to 700 nm (Zhanqing & Moreau 1995), thus neglecting the absorption of the background (i.e. dry and bright bare soil). LUE was empirically modeled on the basis of the optical parameters F_{Syield} and *PRI* to investigate their potential to track physiological variations in the photosynthetic apparatus that determine LUE.

The measured radiometric signal is a function of biochemical, structural and viewing/illumination parameters (Goel 1989). All these factors have to be considered in order to establish a relationship between the optical parameters and LUE. We used a simple approach to account for structural changes in the canopy during the growing season. This approach consists of performing an empirical analysis period by period along the vegetation cycle in a way that it is reasonable to assume that no major structural changes occur within a given period. Therefore, for each of the three measurement periods, a linear transfer function was established between the optical parameter and the LUE derived from the eddy flux data (LUE_{EDDY}).

Validation of the modeled GPP was performed exploiting measured GPP values from EC (GPP_{EDDY}). The footprint of the tower depends on various environmental and surface

conditions as well as the instrumental setup (height of the tower) and can range between a few hectares to a few square-kilometers (Schmid & Lloyd 1999). The area to which the flux measurements are most sensitive, the so called *footprint peak*, is smaller and typically extends up-wind the measurement point for a distance of few hundred meters (Kljun et al. 2004). The results from an analytical footprint model (Hsieh et al. 2000) indicate that the peak footprint is mostly located within the corn field (maximum peak distance of 170 m) and the performed comparison with radiometric measurements within the corn field is hence feasible (Hilker *et al.* 2008a).

3 Results

Measurements of CO_2 exchange and active fluorometry at leaf-level show a physiological limitation of photosynthesis during the days in September. Figure 2A shows LUE over the course of one day (September, 13^{th}) measured at different levels: (1) leaf-level LUE of light reactions of photosynthesis was measured using the clip-on PAM fluorometer (LUE_{PAM}), (2) leaf-level LUE of carbon fixation was measured using the clip-on LICOR gas-exchange analyzer (LUE_{LICOR}), and (3), for comparison, canopy-level LUE of carbon fixation was derived from the eddy flux data (LUE_{EDDY}). Even though leading to different absolute values, the three measurements showed a comparable diurnal course with high LUE during environmentally moderate morning hours, a clear depression of LUE during afternoon, when conditions are dry and hot, and an increase towards the evening, when conditions again become moderate. Additionally, leaf-level LUE began to increase around 12:30 h, while canopy LUE recovery was delayed by about 2 hours (Fig. 2A). We compared photosynthetic rates at the three levels (Fig. 2B): (1) leaf-level electron transport rate at photosystem II was measured using the clip-on PAM fluorometer (ETR_{PAM}), (2) leaf-level CO_2 uptake rate was measured using the clip-on LICOR gas-exchange analyzer (J_{CO_2}), and (3) canopy-level GPP

was derived from the eddy flux data (GPP_{EDDY}). Regardless the used method, maximum rates of photosynthesis occurred between 10:00 h and 12:00 h, when PPFD also reached its maximum. During afternoon, photosynthetic rates decreased and the time shift between leaf and canopy level measurements is observable again: $ETR_{PAM,}$ referring to the very first step of photosynthetic energy conversion (light reaction), decreases first, followed by a decrease in the leaf-level CO_2 uptake rate (J_{CO_2}, dark reactions), and finally also ecosystem GPP_{EDDY} decreased (Fig. 2B).

figure 2

The time shift between leaf and canopy measurements can be explained by the vertical characterization of the canopy showing significant variations of parameters related to photosynthesis (Fig. 3). The canopy was in the beginning of the senescent phase in September and grain-filling was still in progress. Corn canopies in this phenological state are affected by senescing effects spreading in two different directions: a decline of structural and functional parameters from top to bottom and from bottom to top (Tollenaar & Daynard 1978, Valentinuz & Tollenaar 2004). Both directions can be observed with our measurements. The structural parameter *chlorophyll content* was highest for the middle leaves (45-50 µg cm^{-2}) and largely decreases for the upper leaves (20-35 µg cm^{-2}) (Fig 3, left panel). A similar trend was measured for different functional parameters. The highest values for the *maximum assimilation rate of CO_2* (A_{max}) and the *stomatal conductance* (G_s) (Fig. 3 middle panels) were observed for the middle leaves, whereas both parameters declined in upward and downward directions. On the contrary, the *maximum quantum yield of PS II* (F_v/F_M) shows a monotonous decline from the bottom (0.77) to the top (0.72) (Fig. 3 right panel). Lower values in the upper leaves which are more exposed to incident PPFD, together with the overall

absolute value of Fv/Fm (F_v/F_M < 0.77; healthy leaves have a F_v/F_M of 0.83 (Bjorkman & Demmig 1987)) may indicate that the canopy was additionally affected by photoinhibition.

figure 3

Eddy flux data for all days showed that the carbon fixation of plants is mainly determined by the amount of incident photosynthetic active radiation (Fig. 4A), which is in agreement with results documented in the literature (Wofsy et al. 1993).

The assimilation rate in June (highest peak value 50 µmol m^{-2} s^{-1}) was higher than in September (highest peak value 32 µmol m^{-2} s^{-1}). The decrease in September was due to lower PPFD but also due to lower light use efficiency (June: 0.057 mol CO_2 mol^{-1} photons; September: 0.031 mol CO_2 mol^{-1} photons) (Fig. 4B). In fact, seasonal differences in GPP_{EDDY} are not affected only by the incident PPD but also by the phenological state of the crop, which in turn determines leaf area index (LAI) and photosynthetic pigments in the canopy. In June, the canopy was in the growing phase (Chlorophyll content 0.0105 µg m^{-2}, LAI 2.2) while in September it was at the beginning of the senescence phase (Chlorophyll content 0.0093 µg m^{-2}, LAI 2.8).

figure 4

Day courses of GPP_{EDDY} in June were symmetrical around solar noon, while in September GPP_{EDDY} data showed an asymmetry in the diurnal course with a clear depression in the afternoon (Fig. 4A). This phenomenon is often described as ‘midday depression’ and explained with high temperature and high vapor pressure difference (VPD) between air and leaf-tissue that often cause high evaporative demand. This in turn causes stomata to close and results in reduced carbon uptake around noon and early afternoon. Hence, under comparable

illumination conditions the carbon uptake is reduced in the afternoon with respect to the morning hours.

We tested the validity of optical parameters (F_{Syield} and PRI) measured above the canopy for their potential to quantify the dynamic changes in canopy LUE. Therefore, an empirical and linear transfer function between the optical parameters and LUE_{EDDY} was calculated for each time period and position within the field (Fig. 5A, C).

figure 5

The relationships gathered by matching simultaneous measurements of LUE_{EDDY} and optical parameter were weak for both optical parameters in all three periods (Table 2).

table 2

On the experimental basis of the time shift observed for LUE measured at different scales (i.e. leaf and canopy, see Fig.2) we hypothesized that an analogous time shift may exists between canopy LUE (i.e. LUE_{EDDY}) and optical parameters. In order to find this time shift, we systematically adjusted the datasets for the time shift using a cross-correlation approach (Fig. 6). The relationship between the Fs_{yield} and LUE_{EDDY} significantly increased by shifting Fs_{yield} by -1.5 h (figure 5B, D, figure 6 and table 2).

Figure 6

Especially the time shifted data show a stepwise increase of the multiplicative factors of the linear transfer functions between LUE_{EDDY} and F_{Syield} with ongoing senescence (Fig 5B). In

contrast, even on time shifted data, relationships for the PRI were weaker and no systematic trend was found (Fig. 5D).

Once the transfer functions for every single period were defined as above, we employed them in Eq. 7 (i.e. to model LUE) to estimate GPP daily courses of GPP in 30 minute intervals. GPP estimated from fluorescence yield ($GPP_{FSyield}$) showed the best agreement with the measured diurnal courses of GPP_{EDDY}, while using the PRI (GPP_{PRI}) did not yield reasonable estimates of GPP_{EDDY} (Fig. 7 and Table 3).

figure 7

For sake of comparison figure 7 also reports GPP modeled assuming a constant LUE (computed as diurnal average of the LUE_{EDDY} values).

table 3

4 Discussion

The main focus of this study was to evaluate the use of optical parameters for modeling short time responses of photosynthesis and CO_2 assimilation to environmental conditions. Therefore, diurnal courses of F_{Syield} and PRI were acquired and used as proxies for LUE.

Using basic Monteith´s modeling (i.e. constant value for light use efficiency) provided poor results: the amount of fixed CO_2 was underestimated in the morning and strongly overestimated from midday until afternoon. The use of PRI to modulate the LUE did not increase the accuracy of the estimates: the assimilation estimates based on PRI (GPP_{PRI}) did not even track the shape of the measured GPP_{EDDY} (Fig. 6). Sims et al. (2006) or Methy (2000) denote a significance decrease of the relationship between PRI and photosynthesis if

490 measurements were up-scaled from leaf to canopy level. In contrast, a couple of studies show
491 that the PRI is sensitive for diurnal variations of canopy photosynthesis (e.g. (Nichol *et al.*
492 2002, Hall *et al.* 2008)). The situation remains unclear and requires more systematic research.
493 However, Barton and North (2001), Grace et al. (2007), and Hilker et al. (2008a)
494 demonstrated the dependency of the PRI on various structural effects and illumination
495 conditions. Apparently, the diurnal dynamics of photosynthesis tracked with the PRI is
496 affected by canopy structure and observation properties. The superimposition may amplify in
497 stressed, photoinhibited canopies as shown in this study. In such cases, the dynamical
498 adaption of NPQ mechanisms is limited and appears more constant during the day.
499 Nevertheless, our results show that the PRI is to some extent sensitive to seasonal variations,
500 which is in consistency with other works (Nichol *et al.* 2002, Hall *et al.* 2008). Thus, the
501 assumption of decreasing LUE_{EDDY} and PRI with increasing senescence can be confirmed in
502 the seasonal context (Fig. 5C and D). Fluorescence yield, on the other hand, is capable of
503 reproducing the diurnal course of GPP and the prominent midday depression (Fig. 7).
504 The time shift of 1.5 hours between the flux and radiometric data can be mechanistically
505 explained as follows: plant photosynthesis is primarily driven by the meteorological variables
506 *water vapor deficit*, *temperature* and *photosynthetic photon flux density*. The diurnal variation
507 of these variables leads to the midday depression of photosynthesis that is most prominent for
508 C3 species but also present for C4 species (Hirasawa & Hsiao 1999). However, it must be
509 noted that not all the leaves composing the canopy experience the same environmental
510 conditions during the day. For example, top level leaves will receive more radiation than
511 bottom leaves. Moreover, as a result of the vertical gradient in environmental conditions
512 (including radiation, temperature, VPD), the leaves adapt to different biochemical and
513 physiological states, as demonstrated by the vertical characterization of the corn canopy
514 described in Fig. 3. The graph shows that the vertical variability of the meteorological
515 variables leads to different photosynthetic rates and capacities within different layers of the

516 canopy. This basically means that GPP of different canopy layers will respond to
517 environmental conditions at different times during the day. GPP_{EDDY} in contrast will detect
518 the overall response of the canopy.
519 The importance of such observations is confirmed by different models. Chen et al. (1999)
520 show, for example, an improvement of diurnal estimates of canopy photosynthesis using
521 multi-layer models instead of a one-layer model. The improvement was mostly due to the fact
522 that multi-layer models consider the vertical variability of photosynthesis.
523 In our experiment, the observed areas of the canopy differ within the field of view of the eddy
524 flux tower and the spectrometer. The flux tower receives an integrated signal from a huge
525 footprint and the entire vertical canopy. The spectrometer, however, observes the response
526 from the upper canopy. This layer of the canopy is earlier exposed to high light intensities and
527 high VPD than the lower ones. Additionally, the elevated senescence in the upper canopy and
528 effects of photoinhibition leading to a higher stress level in the upper leaves compared to the
529 leaves in the middle canopy (Fig. 3). Hence, it is likely that the stomatal conductance of the
530 upper leaves is reduced earlier during the day than that of the other inner leaves. As a
531 consequence, the modeled GPP based on optical parameters (sensing mainly the upper leaves)
532 will decrease earlier than the measured GPP_{EDDY} from the integrated canopy.
533 This interpretation was supported by analyzing two diurnal courses of another crop (winter
534 wheat) from early May 2008 (data not shown). The canopy was 0.30 m high and the
535 conditions of different vertical layers of the canopy are expected to be more homogeneous.
536 No time discrepancy between the eddy flux measurements and the optical parameters were
537 observed in this case.
538 Besides the mentioned physiological explanation, also micrometeorological considerations
539 can explain the observed time shift. Air masses might remain stored within the canopy some
540 time before being grabbed by turbulent eddies that can be sampled by the eddy covariance
541 technique.

The measured radiometric signal is a function of biochemical, structural and external factors and the absolute value of the derived optical parameters depend on these factors. Barton and North (2001) showed for example the dependency of PRI on LAI, leaf angle distribution (LAD), solar/view angle and soil type. As natural canopies are an assembly of differently oriented leaves, which change their orientation during plant development and as a response to environmental conditions, there is no general function available to transfer PRI or fluorescence yield into LUE (Barton & North 2001). In this study, we used empirical transfer functions to scale the optical parameters to LUE_{EDDY} (Fig. 5). The negative correlation between Fs_{yield} and LUE_{EDDY} seems reasonable as we found some indications for photoinhibition with a F_v/F_M of 0.75, especially for the upper leaves (Fig. 3). Under such photoinhibited circumstances, non-photochemical mechanisms do not vary significantly and, hence, do not dynamically adapt to environmental conditions. In consequence, NPQ appears nearly constant during the day. LUE is reduced as a result of limited photosynthesis in such situations. At the same time, the F_{Syield} increases with increasing amount of incident photons and in consequence, the relationship appears negative (refer (van der Tol *et al.* 2009), for a description based on a mechanistic model).

A change in the slope of the transfer functions between LUE_{EDDY} and Fs_{yield} was observed in the two phenological stages considered. During the process of senescence, the amount of chlorophyll declines. Additionally, a higher stress potential can be expected in September due to unfavorable environmental and meteorological conditions (e.g. dry soils), which result in a stomata closure from late morning until early afternoon. The photosynthetic capacity of the plants is limited and stress occurs due to high light conditions. In such situations, photoprotection mechanisms were up-regulated to dissipate the excessive light and avoid photoinhibition. In the case of chronicle photoinhibition, non-photochemical quenching processes may be limited and an increased amount of light is converted to fluorescence light.

One of the crucial steps in such kind of analysis is the choice of a proper and robust retrieval method. We investigated different methods, e.g. the standard FLD method (Plascyk 1975), the modified method proposed from Maier (2003) and the improved FLD method from Alonso et al. (2008). The absolute values of FS differed for all methods, but each of them provided a similar sensitivity to the diurnal variability of the fluorescence signal. Finally, we decided to use the method proposed from Maier (2003) being most robust and less sensitive to errors occurring during the measurement of the fluorescence signal. We are aware of some of the restrictions of the method, especially the assumption of linearity and maybe a slight sensitivity to bidirectional reflectance effects.

Utilizing fluorescence to model GPP spatial explicit at regional or global scale, however, necessitates investigation on challenging issues. These are i) the precise correction of atmospheric effects that are influencing the measurement of satellite based fluorescence (Guanter *et al.* 2007); ii) a better understanding of the influence of canopy structure at the Fs-signal; iii) contribution of different surface elements to the Fs-signal covered with a remote sensor; iv) impact of changing viewing-illumination geometry to the Fs-signal (Meroni *et al.* 2008b). A further research topic is the physiological relationship between fluorescence and photosynthesis. Various working groups showed a significant relationship between Fs and photosynthesis (van der Tol et al. (2009) as example for modelled data, or Meroni et al. (2008b) as example for experimental studies). However, the existence of NPQ mechanisms may lead to changing relationships between both parameters within one day, between different species and in response to phenological states. The ESA supported global satellite mission for sensing solar-induced fluorescence FLEX (Fluorescence Explorer) is currently under evaluation. Within this framework, the mentioned aspects are subjects of research. For example, the recent availability of an integrated leaf-canopy fluorescence model (ESA, FluorMOD project (Zarco-Tejada *et al.* 2006)), in combination with mechanistic experimental

592 field studies, should provide the necessary base for investigating the mentioned effects in
593 order to up-scale the approach to landscape level.
594
595 **5 Conclusions and Outlook**
596 To our knowledge, this work shows for the first time the modeling of diurnal courses of GPP
597 based on remotely sensed fluorescence yield. We showed that the short time response of a
598 complex physiological process to variable environmental conditions can be tracked reliably
599 with this optical parameter.
600 The correlation analysis between Fs_{Yield} and LUE_{EDDY} highlighted a time discrepancy between
601 the two measurements (Fs_{yield} anticipated LUE_{EDDY} by 1.5 hours). Accounting for this delay
602 was hence to correctly relate eddy flux measurements to remotely sensed estimates of LUE.
603 An explanation of this delay related to the vertical structure of the canopy and to the different
604 footprint sensed by the eddy and spectrometric systems was given. Nevertheless, the influence
605 of the canopy structure on both eddy and spectrometry needs to be investigated in depth to
606 fully understand its influence on GPP estimates from remotely sensed data.
607 We were able to account for the impact of structure on the radiometric signal with a
608 straightforward empirical approach. However, we also anticipate the challenges of applying
609 the promising outcomes of this study over various plant ecosystems to model GPP spatially
610 explicitly from optical parameters and to test its robustness for different environmental
611 factors. Nevertheless we propose the sun-induced fluorescence yield signal being a promising
612 candidate for a remote sensing parameter that can be used over a variety of plant ecosystems
613 to quantify light use efficiency directly.
614 Research in this field is currently strongly supported by the selection of the FLEX mission as
615 one of ESA's candidate missions for a future Earth Explorer (Rascher 2007, Rascher &
616 Pieruschka in press). Several measurement campaigns are currently under way to evaluate the
617 accuracy by which sun-induced fluorescence can be used to quantify photosynthetic

efficiency and stresses (see e.g. http://www.esa.int/esaLP/SEMQACHYX3F_index_0.html). Based on the outcome of these campaigns, it is likely that satellite-based quantification of sun-induced fluorescence yield will become a powerful tool for better understanding spatio-temporal variations of fluorescence yield, photosynthetic efficiency and distribution of plant stresses on a global scale and this way of GPP and carbon uptake.

Acknowledgements

This work was supported by a grant of the European Space Agency (ESA) in the frame of the CEFLES2 campaign (grant No. 20802/07/LG). We also thank Remo Bianchi and Michael Berger for their organizational support. The authors acknowledge Giovanni Agati (CNR-IFAC, Florence), Roberto Colombo (UNIMIB, Milan), Gloria Fernandez, Luis Alonso and Jordi Garcia (RSU, University of Valencia), Alessandro Zaldei and Piero Toscano (CNR-IBIMET, Florence), Jonas Franke (University of Bonn) and Marion Stellmes (University of Trier) for there valuable help during the field campaigns. The authors are also thankful to the two anonymous reviewers who provided constructive comments to improve this manuscript.

635 **Literature**

636 Alonso L, Gómez-Chova L, Vila-Francés J, Amorós-López J, Guanter L, Calpe J, Moreno J
637 (2008) Improved fraunhofer line discrimination method for vegetation fluorescence
638 quantification. *IEEE Geoscience and Remote Sensing Letters (in press),*
639 ASD (2002) *Fieldspec^{tm} pro. Users guide.* Analytical Spectral Devices, Inc., Boulder (CO).
640 Aubinet M, Grelle A, Ibrom A*, et al.* (2000) Estimates of the annual net carbon and water
641 exchange of forests: The euroflux methodology. In: *Advances in ecological research,*
642 *vol 30* Vol. 30, pp. 113-175.
643 Baker NR (2008) Chlorophyll fluorescence: A probe of photosynthesis in vivo. *Annual*
644 *Reviews - Plant Biology,* **59**, 89-113.
645 Baldocchi D, Falge E, Gu LH*, et al.* (2001) Fluxnet: A new tool to study the temporal and
646 spatial variability of ecosystem-scale carbon dioxide, water vapor, and energy flux
647 densities. *Bulletin of the American Meteorological Society,* **82**, 2415-2434.
648 Baldocchi DD (2003) Assessing the eddy covariance technique for evaluating carbon dioxide
649 exchange rates of ecosystems: Past, present and future. *Global Change Biology,* **9**,
650 479-492.
651 Barton CVM, North PRJ (2001) Remote sensing of canopy light use efficiency using the
652 photochemical reflectance index - model and sensitivity analysis. *Remote Sensing of*
653 *Environment,* **78**, 264-273.
654 Bilger W, Schreiber U, Bock M (1995) Determination of the quantum efficiency of
655 photosystem ii and of non-photochemical quenching of chlorophyll fluorescence in the
656 field. *Oecologia,* **102**, 425-432.
657 Bjorkman O, Demmig B (1987) Photon yield od o-2 evolution and chlorophyll fluorescence
658 characteristics at 77-k among vascular plants of diverse origins. *Planta,* **170**, 489-504.
659 Carter GA, Theisen AF, Mitchell RJ (1990) Chlorophyll fluorescence measured using the
660 fraunhofer line-depth principle and relationship to photosynthetic rate in the field.
661 *Plant Cell and Environment,* **13**, 79-83.
662 Chen JM, Liu J, Cihlar J, Goulden ML (1999) Daily canopy photosynthesis model through
663 temporal and spatial scaling for remote sensing applications. *Ecological Modelling,*
664 **124**, 99-119.
665 Cohen WB, T.K. M, Yang ZQ (2003) Comparisons of land cover and lai estimates derived
666 from etm plus and modis for four sites in north america: A quality assessment of
667 2000/2001 provisional modis products *Remote Sensing of Environment,* **88**, 256-270.
668 Coops NC, Black TA, Jassal RPS, Trofymow JAT, Morgenstern K (2007) Comparison of
669 modis, eddy covariance determined and physiologically modelled gross primary
670 production (gpp) in a douglas-fir forest stand. *Remote Sensing of Environment,* **107**,
671 385-401.
672 Demmig-Adams B, Adams WW (1996) The role of xanthophyll cycle carotenoids in the
673 protection of photosynthesis. *Trends in Plant Science,* **1**, 21-26.
674 Drolet GG, Middleton EM, Huemmrich KF*, et al.* (2008) Regional mapping of gross light-use
675 efficiency using modis spectral indices. *Remote Sensing of Environment,* **112**, 3064-
676 3078.
677 Ehleringer J (1981) Leaf absorptances of mohave and sonoran desert plants. *Oecologia,* **49**
678 366-370.
679 Eiden M, van der Linden S, Schween J*, et al.* (2007) In: *10th ISPMSRS*. Davos, Swizerland.
680 Field CB, Randerson JT, Malmstrom CM (1995) Global net primary production - combining
681 ecology and remote sensing. *Remote Sensing of Environment,* **51**, 74-88.
682 Franck F, Juneau P, Popovic R (2002) Resolution of the photosystem i and photosystem ii
683 contributions to chlorophyll fluorescence of intact leaves at room temperature.
684 *Biochimica Et Biophysica Acta-Bioenergetics,* **1556**, 239-246.

685 Freedman A, Cavender-Bares J, Kebabian PL, Bhaskar R, Scott H, Bazzaz FA (2002) Remote
686 sensing of solar-excited plant fluorescence as a measure of photosynthetic rate.
687 *Photosynthetica,* **40**, 127-132.
688 Gamon JA, Filella I, Penuelas J (1993) The dynamic 531-nanometer reflectance signal: A
689 survey of twenty angiosperm species. In: *Photosynthetic responses to the environment*
690 (eds Yamamoto HY, Smith CM), pp. 172-177. American Society of Plant
691 Physiologists, Rockville.
692 Gamon JA, Penuelas J, Field CB (1992) A narrow-waveband spectral index that tracks
693 diurnal changes in photosynthetic efficiency. *Remote Sensing of Environment,* **41**, 35-
694 44.
695 Genty B, Briantais JM, Baker NR (1989) The relationship between the quantum yield of
696 photosynthetic electron-transport and quenching of chlorophyll fluorescence.
697 *Biochimica Et Biophysica Acta,* **990**, 87-92.
698 Goel NS (1989) Inversion of canopy reflectance models for estimation of biophysical
699 parameters from reflectance data. In: *Theory and applications of optical remote*
700 *sensing* (ed Asrar G), pp. 205-251. Wiley & Sons, New York.
701 Goetz SJ, Prince SD (1999) Modelling terrestrial carbon exchange and storage: Evidence and
702 implications of functional convergence in light-use efficiency. In: *Advances in*
703 *ecological research, vol 28* Vol. 28, pp. 57-92.
704 Goulden ML, Munger JW, Fan SM, Daube BC, Wofsy SC (1996) Measurements of carbon
705 sequestration by long-term eddy covariance: Methods and a critical evaluation of
706 accuracy. *Global Change Biology,* **2**, 169-182.
707 Govindjee (1995) 63 years since kautsky chlorophyll-a fluorescence *Australian Journal of*
708 *Plant Physiology,* **22**, 711-711.
709 Govindjee (2004) Chlorophyll a fluorescence: A bit of basics and history. In: *Chlorophyll a*
710 *fluorescence: A signature of photosynthesis. Advances in photosynthesis and*
711 *respiration* Vol. 19 (eds Papageorgiou GC, Govindjee), pp. 1-42. Springer, Dordrecht.
712 Grace J, Nichol C, Disney M, Lewis P, Quaife T, Bowyer P (2007) Can we measure
713 terrestrial photosynthesis from space directly, using spectral reflectance and
714 fluorescence? *Global Change Biology,* **13**, 1484-1497.
715 Guanter L, Alonso L, Gomez-Chova L, Amoros-Lopez J, Vila J, Moreno J (2007) Estimation
716 of solar-induced vegetation fluorescence from space measurements. *Geophysical*
717 *Research Letters,* **34**, doi: 10.1029/2007GL029289.
718 Guo JM, Trotter CM (2004) Estimating photosynthetic light-use efficiency using the
719 photochemical reflectance index: Variations among species. *Functional Plant Biology,*
720 **31**, 255-265.
721 Hall FG, Hilker T, Coops NC*, et al.* (2008) Multi-angle remote sensing of forest light use
722 efficiency by observing pri variation with canopy shadow fraction. *Remote Sensing of*
723 *Environment,* **112**, 3201-3211.
724 Heinsch FA, Reeves M, Votava P*, et al.* (2002).
725 Hilker T, Coops NC, Hall FG, Black TA, Wulder MA, Nesic Z, Krishnan P (2008a)
726 Separating physiologically and directionally induced changes in pri using brdf models.
727 *Remote Sensing of Environment,* **112**, 2777-2788.
728 Hilker T, Coops NC, Wulder MA, Black AT, Guy RD (2008b) The use of remote sensing in
729 light use efficiency based models of gross primary production: A review of currant
730 status and future requirements. *Science of the Total Environment,* **404**, 411-423.
731 Hirasawa T, Hsiao TC (1999) Some characteristics of reduced leaf photosynthesis at midday
732 in maize growing in the field. *Field Crops Research,* **62**, 53-62.
733 Hsieh CI, Katul GG, Chi TW (2000) An approximate analytical model for footprint
734 estimation of scalar fluxes in thermally stratified atmospheric flows. *Advances in*
735 *Water Resources,* **23**, 765-772.

Janzen HH (2004) Carbon cycling in earth systems - a soil science perspective. *Agriculture Ecosystems & Environment,* **104**, 399-417.
Kljun N, Kastner-Klein P, Fedorovich E, Rotach MW (2004) Evaluation of lagrangian footprint model using data from wind tunnel convective boundary layer. *Agricultural and Forest Meteorology,* **127**, 189-201.
Lichtenthaler HK (1987) Chlorophylls and carotenoids - pigments of photosynthetic biomembranes. *Methods in Enzymology,* **148**, 350-382.
Lichtenthaler HK, Rinderle U (1988) The role of chlorophyll fluorescence in the detection of stress conditions in plants. *Crc Critical Reviews in Analytical Chemistry,* **19**, S29-S85.
Louis J, Ounis A, Ducruet JM*, et al.* (2005) Remote sensing of sunlight-induced chlorophyll fluorescence and reflectance of scots pine in the boreal forest during spring recovery. *Remote Sensing of Environment,* **96**, 37-48.
Maier SW, Günther KP, Stellmes M (2003) Sun-induced fluorescence: A new tool for precision farming. In: *Digital imaging and spectral techniques: Applications to precision agriculture and crop physiology* Vol. 66 (eds McDonald M, Schepers J, Tartly L, van Toai T, Major D), pp. 209-222. ASA Special Publication
Maxwell K, Johnson GN (2000) Chlorophyll fluorescence - a practical guide. *Journal of Experimental Botany,* **51**, 659-668.
Meroni M, Colombo R (2006) Leaf level detection of solar induced chlorophyll fluorescence by means of a subnanometer resolution spectroradiometer. *Remote Sensing of Environment,* **103**, 438-448.
Meroni M, Picchi V, Rossini M*, et al.* (2008a) Leaf level early assessment of ozone injuries by passive fluorescence and photochemical reflectance index. *International Journal of Remote Sensing,* **29**, 5409-5422.
Meroni M, Rossini M, Picchi V, Panigada C, Cogliati S, Nali C, Colombo R (2008b) Assessing steady-state fluorescence and pri from hyperspectral proximal sensing as early indicators of plant stress: The case of ozone exposure. *Sensors,* **8**, 1740-1754.
Methy M (2000) Analysis of photosynthetic activity at the leaf and canopy levels from reflectance measurements: A case study. *Photosynthetica,* **38**, 505-512.
Monteith JL (1972) Solar-radiation and productivity in tropical ecosystems. *Journal of Applied Ecology,* **9**, 747-766.
Monteith JL (1977) Climate and efficiency of crop production in britain. *Philosophical Transactions of the Royal Society of London Series B-Biological Sciences,* **281**, 277-294.
Moya I, Camenen L, Evain S*, et al.* (2004) A new instrument for passive remote sensing 1. Measurements of sunlight-induced chlorophyll fluorescence. *Remote Sensing of Environment,* **91**, 186-197.
Nichol C, Lloyd J, Shibistova O*, et al.* (2002) Remote sensing of photosynthetic-light-use efficiency of a siberian boreal forest. *Tellus Series B-Chemical and Physical Meteorology,* **54**, 677-687.
Ozanne CMP, Anhuf D, Boulter SL*, et al.* (2003) Biodiversity meets the atmosphere: A global view of forest canopies. *Science,* **301**, 183-186.
Papale D, Valentini A (2003) A new assessment of european forests carbon exchanges by eddy fluxes and artificial neural network spatialization. *Global Change Biology,* **9**, 525-535.
Plascyk JA (1975) Mk ii fraunhofer line dicsriminator (fld-ii) for airborne and orbital remote-sensing of solar-stimulated luminescence. *Optical Engineering,* **14**, 339-346.
Rascher U (2007) Flex - fluorescence explorer: A remote sensing approach to quantify spatio-temporal variations of photosynthetic efficiency from space. *Photosynthesis Research,* **91**, 293-294.

786 Rascher U, Nedbal L (2006) Dynamics of photosynthesis in fluctuating light - commentary.
787 *Current Opinion in Plant Biology,* **9**, 671-678.
788 Rascher U, Nichol CL, Small C, Hendricks L (2007) Monitoring spatio-temporal dynamics of
789 photosynthesis with a portable hyperspectral imaging system. *Photogrammetric*
790 *Engineering and Remote Sensing,* **73**, 45-56.
791 Rascher U, Pieruschka R (in press) Spatio-temporal variations of photosynthesis - the
792 potential of optical remote sensing to better understand and scale light use efficiency
793 and stresses of plant ecosystems. *Precision Agriculture,*
794 Reichstein M, Falge E, Baldocchi D*, et al.* (2005) On the separation of net ecosystem
795 exchange into assimilation and ecosystem respiration: Review and improved
796 algorithm. *Global Change Biology,* **11**, 1424-1439.
797 Reichstein M, Tenhunen JD, Roupsard O*, et al.* (2002) Severe drought effects on ecosystem
798 co2 and h2o fluxes at three mediterranean evergreen sites: Revision of current
799 hypotheses? *Global Change Biology,* **8**, 999-1017.
800 Running SW, Nemani RR, Heinsch FA, Zhao MS, Reeves M, Hashimoto H (2004) A
801 continuous satellite-derived measure of global terrestrial primary production.
802 *Bioscience,* **54**, 547-560.
803 Schmid HP, Lloyd CR (1999) Spatial representativeness and the location bias of flux
804 footprints over inhomogeneous areas. *Agricultural and Forest Meteorology,* **93**, 195-
805 209.
806 Schreiber U, Bilger W (1993) Progress in chlorophyll fluorescence research: Major
807 developments during the past years in retrospect. *Progress in Botany,* **53**, 151-173.
808 Schreiber U, Bilger W, C. N (1995) Chlorophyll fluorescence as a nonintrusive indicator for
809 rapid assessment of in vivo photosynthesis. In: *Ecophysiology of photosynthesis* (eds
810 Schulze ED, Caldwell MM), pp. 49-70. Springer, Berlin, Heidelberg, Nwe York.
811 Schulze ED, Caldwell MM (Eds.) (1995) *Ecophysiology of photosynthesis. Ecological*
812 *studies,* Springer Verlag, Berlin, Heidelberg.
813 Schurr U, Walter A, Rascher U (2006) Functional dynamics of plant growth and
814 photosynthesis - from steady-state to dynamics - from homogeneity to heterogeneity.
815 *Plant Cell and Environment,* **29**, 340-352.
816 Sims DA, Luo HY, Hastings S, Oechel WC, Rahman AF, Gamon JA (2006) Parallel
817 adjustments in vegetation greenness and ecosystem co2 exchange in response to
818 drought in a southern california chaparral ecosystem. *Remote Sensing of Environment,*
819 **103**, 289-303.
820 Tollenaar M, Daynard TB (1978) Leaf senescence in short-season maize hybrids. *Canadian*
821 *Journal of Plant Science,* **58**, 869-874.
822 Turner DP, Ritts WD, Cohen WB*, et al.* (2003a) Scaling gross primary production (gpp) over
823 boreal and deciduous forest landscapes in support of modis gpp product validation.
824 *Remote Sensing of Environment,* **88**, 256-270.
825 Turner DP, Ritts WD, Cohen WB*, et al.* (2005) Site-level evaluation of satellite-based global
826 terrestrial gross primary production and net primary production monitoring. *Global*
827 *Change Biology,* **11**, 666-684.
828 Turner DP, Urbanski S, Bremer D, Wofsy SC, Meyers T, Gower ST, Gregory M (2003b) A
829 cross-biome comparison of daily light use efficiency for gross primary production.
830 *Global Change Biology,* **9**, 383-395.
831 Valentinuz OR, Tollenaar M (2004) Vertical profile of leaf senescence during the grain-filling
832 period in older and newer maize hybrids. *Crop Science,* **44**, 827-834.
833 van der Tol C, Verhoef W, Rosema A (2009) A model for chlorophyll fluorescence and
834 photosynthesis at leaf scale. *Agricultural and Forest Meteorology,* **149**, 96-105.
835 WALZ (2008).

836 Webb EK, Pearman GI, Leuning R (1980) Correction of flux measurements for density
837 effects due to heat and water-vapour transfer. *Quarterly Journal of the Royal*
838 *Meteorological Society,* **106**, 85-100.
839 Wofsy SC, Goulden ML, Munger JW*, et al.* (1993) Net exchange of co2 in a midlatitude
840 forest. *Science,* **260**, 1314-1317.
841 Zarco-Tejada PJ, Miller JR, Pedros R, Verhoef W, Berger M (2006) Fluormodgui v3.0: A
842 graphic user interface for the spectral simulation of leaf and canopy chlorophyll
843 fluorescence. *Computers & Geosciences,* **32**, 577-591.
844 Zhanqing L, Moreau L (1995) A new approach for remote sensing of canopy-absorbed
845 photosynthetically active radiation. I: Total surface absorption. *Remote Sensing of*
846 *Environment,* **55**, 175-191.
847
848
849

Tables

Table 1. Summary of available day courses of radiometric measurements of a corn canopy.

Period	Date	Time window (hh:mm, UTC)
1	30. June	14:30-19:30
2	05. September	10:30-18:00
2	06. September	09:00-17:00
2	07. September	09:30-18:00
3	12. September	09:00-16:50

Table 2: Statistical parameters characterizing the relationship of LUE_{EDDY} and optical parameters (F_{Syield} = fluorescence yield; F_{Syield}_time = time shifted F_{Syield}; PRI = Photochemical Reflectance Index; PRI_time = time shifted PRI, p-value = significance of correlation; n = number of measurements).

		June	Sep (5.-7.)	Sep (12.)	average
R^2	F_{Syield}	0.04	0.17	0.14	0.12
	F_{Syield}_time	0.56	0.46	0.59	0.54
	PRI	0.13	0.02	0.65	0.27
	PRI_ time	0.44	0.04	0.19	0.22
RMSE	F_{Syield}	0.026	0.005	0.004	0.0117
	F_{Syield}_time	0.013	0.005	0.001	0.0063
	PRI	0.029	0.017	0.006	0.0173
	PRI_ time	0.060	0.018	0.003	0.0270
p-value	F_{Syield}	0.99	0.06	0.38	0.48
	F_{Syield}_time	0.40	0.96	0.46	0.60
	PRI	0.98	0.30	0.99	0.76
	PRI_time	0.95	0.94	0.86	0.92
n	F_{Syield}	11	49	15	
	F_{Syield}_time	8	31	14	
	PRI	11	43	15	
	PRI_time	8	31	14	

Table 3: Statistical parameters characterizing the relationship of modeled and measured GPP (F_{Syield} = fluorescence yield; F_{Syield}_time = time shifted F_{Syield}; PRI = Photochemical Reflectance Index; PRI_time = time shifted PRI; const. LUE = constant Light Use Efficiency).

		June	Sep (5.-7.)	Sep (12.)	avg.
R^2	const. LUE	0.91	0.92	0.95	0.93
	F_{Syield}	0.30	0.83	0.89	0.67
	F_{Syield}_ time	0.83	0.97	0.98	0.93
	PRI	0.20	0.05	0.52	0.26
	PRI_ time	0.52	0.34	0.87	0.58
RMSE	const. LUE	4.42	2.51	1.48	2.80
	F_{Syield}	12.40	2.75	2.15	5.77
	F_{Syield}_time	4.55	1.91	0.97	2.48
	PRI	13.20	11.40	3.15	9.25
	PRI_time	7.39	10.94	7.98	8.77

figure captions

Figure 1: Position and dimension of spectrometer footprint (S 1 to 4) for a corn at average canopy height. The position of the white reference panel (WR) is also indicated.

Figure 2: Comparison of diurnal courses of leaf and canopy LUE and GPP of corn at the 13th of September. A: incident PPFD and LUE estimated from different sources: canopy level eddy flux measurements, LUE_{EDDY}, leaf level gas exchange, LUE_{LICOR}, and leaf level active fluorometry, LUE_{PAM}. B: production related information as estimated from eddy flux measurements, GPP_{EDDY}, gas exchange, JCO_2, and active-fluorometry, ETR_{PAM}.

Figure 3: Mean vertical distribution (n=3 plants) of chlorophyll, maximum assimilation rate (A_{max}), stomatal conductance (G_s), and maximum quantum yield of PSII (F_v/F_m) for a senescent corn plants. Horizontal bars referrer to +/- 1 standard deviation. Vertical profiles were collected at the 13th of September and are expressed in term of leaf number, first and 8th leaves being the uppermost and the lowermost, respectively. The plant drawing on the right indicates the leaf vertical position. The decline of parameters from middle to top and middle to bottom is due to senescence (refer the text above for an explanation).

Figure 4: Diurnal courses of GPP_{EDDY} (continuous curve, A (top)) and LUE_{EDDY} (continuous curve, B (bottom)) derived from eddy-flux measurements during the three measurement periods. Incident PPFD is reported for reference (dashed curve).

Figure 5: Relationship between LUE_{EDDY} and optical parameters (fluorescence yield and PRI). A,C: Relationship without time shift. B,D: with time shift. Period 1 corresponds to the 30th of June, period 2 to the 5th – 7th of September and period 3 to the 12th of September

889 Figure 6: Coefficients of determination (R) for cross-correlation based time shift analysis.
890 F_{Syield} were shifted against fixed LUE_{EDDY} data.

891 Figure 7: Diurnal courses of modeled and measured GPP_{EDDY} signal. A: $GPP_{FSyield}$ based on
892 fluorescence yield. B: GPP_{PRI} based on PRI. GPP_{const} refers to GPP modeled with a
893 constant LUE.

894 Figure 1

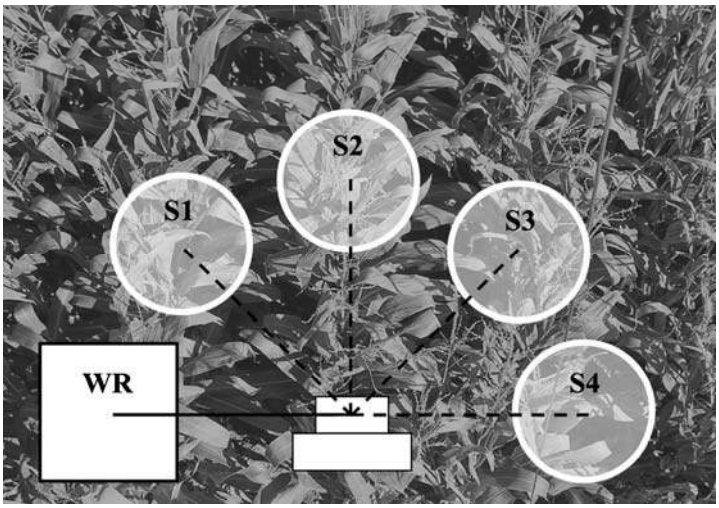

895

896

897

898

899

900

901

902

903

904

905

906

907

908

909

910

911 Figure 2

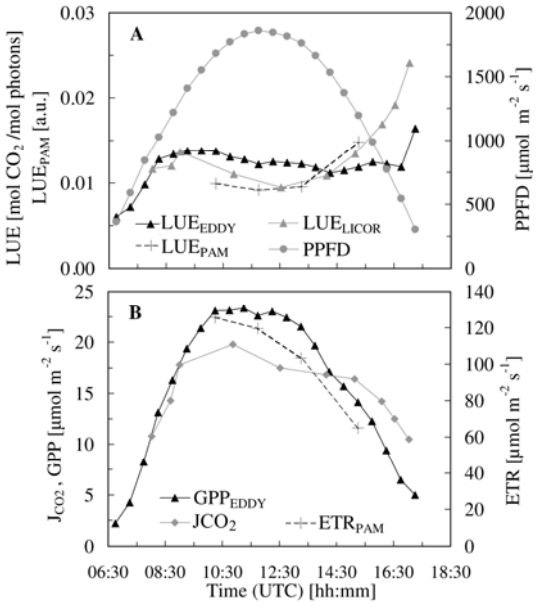

912

913

914

915

916

917

918

919

920

921

922

923

924

925

926

927 Figure 3

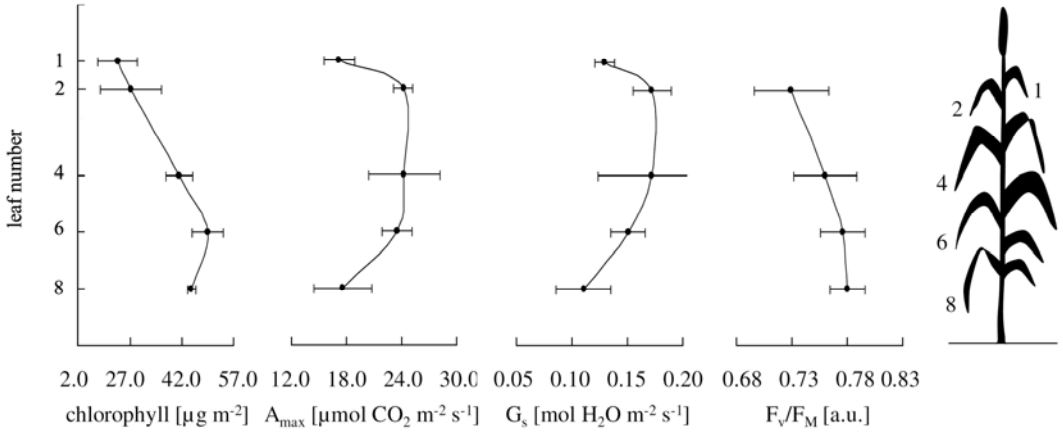

928

929

930

931

932

933

934

935

936

937

938

939

940

941

942

943

944

945 Figure 4

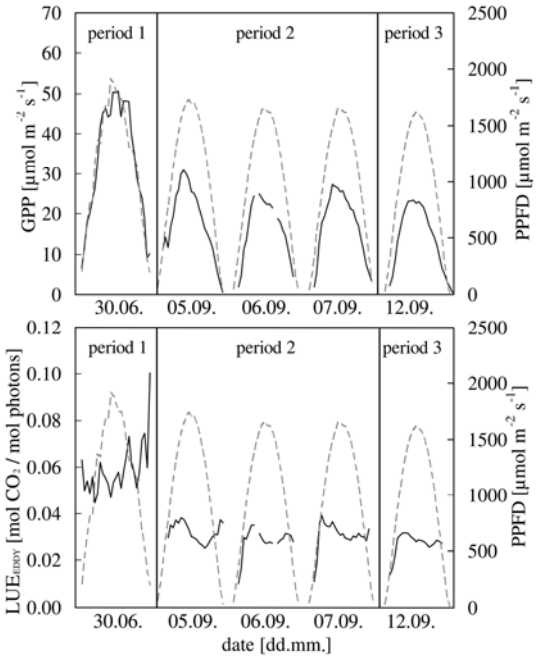

946

947

948

949

950

951

952

953

954

955

956

957 Figure 5

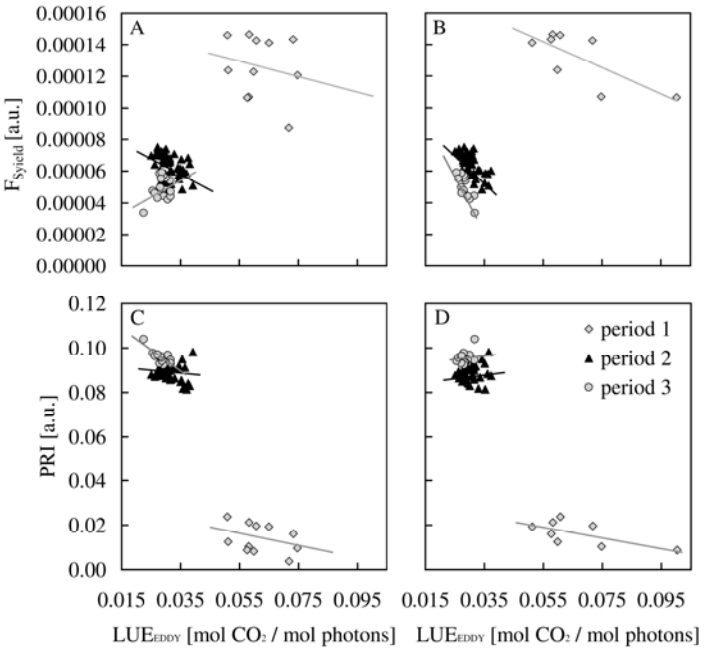

958

959

960

961

962

963

964

965

966

967 Figure 6

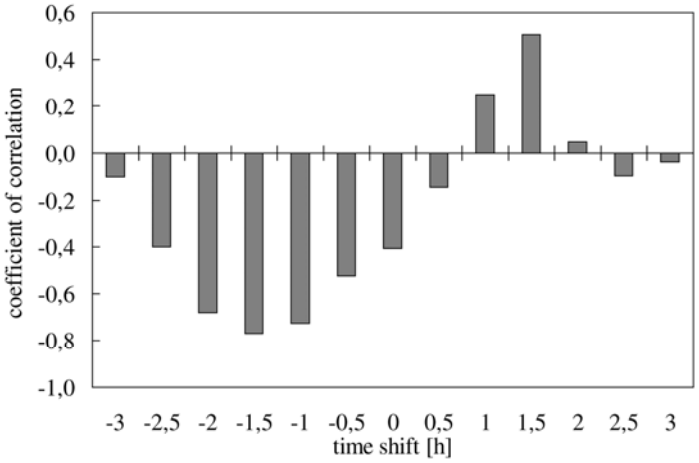

968

969

970

971

972

973

974

975

976

977

978

979

980

981

982

983

984

985

986

987 Figure 7

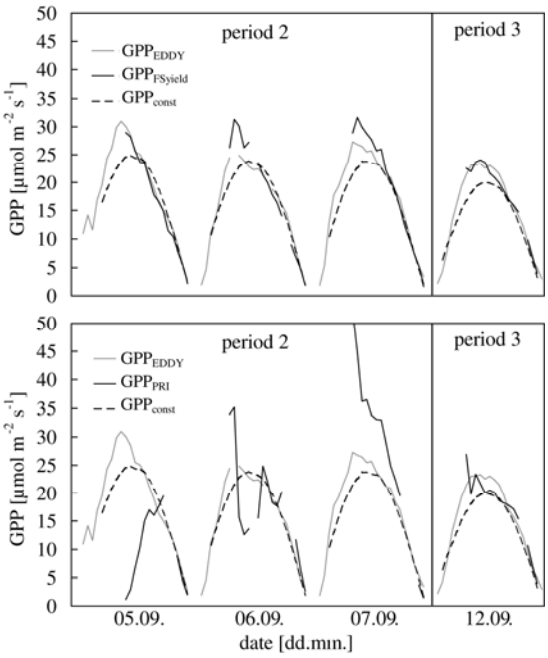

988

989